

LANDMARK-BASED ROBOT NAVIGATION

ANTHONY LAZANAS

lazanas@flamingo.stanford.edu

JEAN-CLAUDE LATOMBE

latombe@cs.stanford.edu

ROBOTICS LABORATORY

DEPARTMENT OF COMPUTER SCIENCE

STANFORD UNIVERSITY, STANFORD, CA 94305, USA

Abstract

Achieving goals despite uncertainty in control and sensing may require robots to perform complicated motion planning and execution monitoring. This paper describes a reduced version of the general planning problem in the presence of uncertainty and a complete polynomial algorithm solving it. The planner computes a guaranteed plan (for given uncertainty bounds) by backchaining omnidirectional backprojections of the goal until one fully contains the set of possible initial positions of the robot. The algorithm assumes that landmarks are scattered across the workspace, that robot control and position sensing are perfect within the fields of influence of these landmarks (the regions in which the landmarks can be sensed by the robot), and that control is imperfect and sensing null outside these fields. The polynomiality and completeness of the algorithm derive from these simplifying assumptions, whose satisfaction may require the robot and/or its workspace to be specifically engineered. This leads us to view robot/workspace engineering as a means to make planning problems tractable. A computer program embedding the planner was implemented, along with navigation techniques and a robot simulator. Several examples run with this program are presented in this paper. Non-implemented extensions of the planner are also discussed.

Acknowledgments: This research was partially funded by DARPA contract DAAA21-89-c0002 and ONR contract N00014-92-J-1809. The authors also thank Leo Guibas for his encouragements and comments.

1. INTRODUCTION

To operate in the real world robots must deal with errors in control and sensing. Several motion planners have been proposed which address this issue (e.g., [24, 32, 11, 20, 16, 25, 27, 12]). Many of them, however, embed tacit or unclear assumptions, causing them to be unreliable in practice.

In this paper, like in [25, 27, 12], we represent uncertainty by bounded regions describing ranges of errors. A *correct* plan is one whose execution is guaranteed to achieve the goal, whenever actual errors (at execution time) are within the uncertainty bounds. A *sound* planner is one which only generates correct plans. A *complete* planner is one which generates a correct plan whenever one exists, and returns failure otherwise. Very few complete planners have been proposed so far. Most of them take exponential time in some measure of the size of the input problem (e.g., [5, 9]), which makes them virtually inapplicable. In fact, it has been shown that these planners attack problems which are inherently intractable [4].

In this paper we achieve polynomiality by both making assumptions in the problem formulation that eliminate the source of intractability, and using algorithmic techniques that take advantage of these assumptions. The key underlying notion is that of a landmark area, an “island of perfection” in the robot configuration space where we consider position sensing and motion control to be fully accurate. Outside any such area, we assume that control is imperfect and position sensing null. This notion of a landmark area approximately corresponds to the “field of influence” of a physical feature: if the robot is in this field, it can sense and identify the feature, and use this information to determine its position with high accuracy (actually, we assume full accuracy). A feature may be pre-existing (e.g., the corner made by two walls) or specifically provided to help robot navigation (e.g., a radio beacon or a magnetic device buried in the ground).

Given a set of landmark areas scattered across configuration space, a set of obstacles with which the robot should not collide, an initial region where the robot is known to be prior to execution, and a goal region where we would like the robot to go, the planning problem is to generate a set of motion commands whose execution guarantees that the robot will move into the goal and stop there. Our planning algorithm solves this problem by iteratively constructing a growing set of landmark areas from which the robot can reliably attain the goal. This set initially contains the landmark areas intersecting the goal region. Then new landmark areas are added, from which the robot can reliably attain landmark areas already in the set by executing a single move. The algorithm terminates successfully as soon as it is possible for the robot to attain some landmark area (any one) in this set by a single move from the initial region. It terminates with failure when no new landmark areas can be added to the set and the condition for success is still unsatisfied.

The algorithm constructs the set of landmark areas from which the robot can reliably attain the goal by computing omnidirectional backprojections. The directional backprojection of a set of landmark areas, for a given direction of motion d , is the largest region in configuration space from which the robot is guaranteed to attain one of these areas by moving along d , despite control uncertainty. The omnidirectional backprojection is the disjoint union of directional backprojections over all possible directions of motion, indexed by the direction of motion. For a robot represented as a point in the plane, we show that the omnidirectional backprojection is sufficiently represented, as far as planning is concerned, by a finite number of directional backprojections. The planner derived from this result is complete. Its time complexity is polynomial in the number and complexity of the landmark areas and the obstacles. The plans it generates minimize the number of motions that have

to be executed in the worst case.

Landmarks require the workspace to include appropriate features and the robot to be equipped with sensors able to detect them. Our planning algorithm thus illustrates the interplay between engineering and algorithmic complexity in robotics. As software becomes more critical in modern robots, the importance of this interplay will increase. The tractability of robot programming will more and more be a major consideration in robot design and workspace engineering. The question is not “How can we avoid engineering?”, but “How can we reduce its cost?” Interestingly, once a motion plan has been generated by our planner, the assumption that control and sensing are perfect in landmark areas can be relaxed to some extent, while keeping the plan correct. Furthermore, we will show that simple variations of our planner can handle other sorts of landmark areas that do not require perfect sensing and control, without losing completeness and polynomiality.

In Section 2 (RELATED WORK) we relate our work to previous research. In Section 3 (PLANNING PROBLEM) we precisely state the class of problems solved by our planner and we illustrate this statement with an example. In Section 4 (DIRECTIONAL BACKCHAINING) we present a first-cut planning method based on the concept of directional backprojection. However, this method does not provide an efficient way to select directions of motion. In Section 5 (OMNIDIRECTIONAL BACKCHAINING) we address this issue and we present the actual planning algorithm. In Section 6 (EXPERIMENTAL RESULTS) we show a series of examples run with the implemented planner. For simplification, Sections 4 through 6 assume that there are no obstacles in the robot’s workspace. In Section 7 (DEALING WITH OBSTACLES) we extend the planning method to deal with obstacles, and we present additional experimental results. In Section 8 (DISCUSSION AND EXTENSIONS) we discuss our assumptions and we describe non-implemented extensions of the planner aimed at eliminating the most restrictive ones.

2. RELATED WORK

Motion planning with uncertainty has been a research topic in robotics for almost two decades. Various approaches have been proposed, including skeleton refinement [24, 32], inductive learning from experiments [11], iterative removal of contacts [20, 16], and preimage backchaining [25, 27, 12]. The first three of these approaches operate in two phases: a motion plan is first generated assuming no uncertainty and then transformed to deal with uncertainty. Instead, preimage backchaining takes uncertainty into account throughout the whole planning process. It can thus tackle problems where uncertainty shapes the structure of a plan to the extent that it cannot be generated by transforming an initial one produced under the no-uncertainty assumption. Our work is a direct continuation of a series of work on preimage backchaining. We focus most of the following discussion on this series.

Preimage backchaining considers the following class of motion planning problems [25]: A plan is a sequence (more generally, an algorithm) of motion commands, each defined by a commanded direction of motion d and a termination condition **TC**. When the robot executes such a command in free space, it moves along a direction contained at each instant in a cone

of half-angle θ about d and stops as soon as **TC** becomes true. (In contact with an obstacle, the robot may stop or slide, depending on the particular control law that is used. In this paper we will simply forbid contacts with obstacles, though our algorithm can be easily adapted to handle compliant motions as well.) The angle θ is the largest expected control error and models the directional uncertainty of the robot. The termination condition **TC** is a boolean function of sensory data s . At any one time, these data measure physical parameters (e.g., the robot position) with some error. The actual parameter vector lies anywhere in a region $\mathcal{U}(s)$ modeling the robot's sensory uncertainty. A planning problem is specified by a workspace model, an initial region, a goal region, the directional uncertainty θ , and the sensing uncertainty \mathcal{U} .

The above problem formulation admits many variants. For example, one may introduce time and consider uncertainty in the robot velocity, allowing the construction of more sophisticated termination conditions [27, 12]. The workspace model (e.g., the location and the shape of the obstacles) may also be subject to errors, yielding a third type of uncertainty [8]. For the sake of simplicity we will not discuss these variants here (see [18]).

The preimage of a goal region for a given motion command $\mathbf{M} = (d, \mathbf{TC})$ is the set of all points in the robot's configuration space such that if the robot starts executing the command from any one of these points, it is guaranteed to reach the goal and stop in it. Preimage backchaining consists of constructing a sequence of motion commands \mathbf{M}_i , $i = 1, \dots, n$, such that, if P_n is the preimage of the goal for \mathbf{M}_n , P_{n-1} the preimage of P_n for \mathbf{M}_{n-1} , and so on, then P_1 contains the initial region.

One source of difficulty in computing preimages is the possible interaction between goal reachability and goal recognizability. The robot must both reach the goal (despite directional uncertainty) and stop in the goal (despite sensing uncertainty). Goal recognition, hence the termination condition of a command, may depend on the region from where the command is executed. This region, which is precisely the preimage of the goal for that command, also depends on the termination condition. This recursive dependence was noted in [25]. Nevertheless, Canny [5] described a complete planner with very few restrictive assumptions in it. This planner generates an r -step plan by reducing the input problem to deciding the satisfiability of a semi-algebraic formula with $2r$ alternating existential and universal quantifiers. Such a decision takes double exponential time in r . Moreover, the smallest r for which a plan may exist grows with the complexity of the environment. Actually, various forms of the above motion planning problem have been proven intrinsically hard [4, 28].

At the expense of completeness, Erdmann [12] suggested that goal reachability and recognizability be treated separately by identifying a subset of the goal, called a kernel, such that when this subset is attained, goal achievement can be recognized (by **TC**) independently of the way it has been achieved. He defined the backprojection of a region R for a direction of motion d as the set of all points such that, if the robot moves along d with directional uncertainty θ , starting at any one of these points, it is guaranteed to reach R . He proposed an $O(n \log n)$ algorithm to compute backprojections in the plane when the obstacles are polygons bounded by n edges. Hence, a preimage of a goal can be computed as the backprojection of its kernel. An implemented planner based on this technique is described

in [19].

Once the kernel of a goal has been identified, a remaining issue is the selection of the commanded direction of motion to attain this kernel, since the backprojection of the kernel varies when the direction changes. The planner described in [19] only considers a finite number of regularly spaced directions; hence, it is incomplete, and usually not very efficient. Donald [9] considered the disjoint union of backprojections of a region R over all possible directions of motion. For a point robot moving in the plane, he showed that this set is sufficiently described by a polynomial number of backprojections. He used this result to propose an $O(n^4 \log n)$ algorithm to generate one-step (single motion command) plans. Briggs [2] reduced the time complexity of this algorithm to $O(n^2 \log n)$. Hutchinson and Fox [17, 14] extended the algorithm to exploit visual constraints and allow visual compliant motions.

One remaining difficulty to construct a multi-step planner is backchaining. The difficulty comes from the fact that backchaining introduces a twofold variation: when the commanded direction of motion varies, both the backprojection of the current kernel and the kernel of this backprojection (which will be used at the next backchaining iteration) vary. In this paper we deal with this difficulty by introducing landmark areas. We show that backchaining is then reduced to iteratively computing a relatively small set of backprojections for a growing set of landmark regions. This result directly yields a polynomial planning algorithm. This planner is also complete relative to a well-defined class of problems. Previously, Friedman [15] had proposed another polynomial multi-step planner for a compliant point robot in a polygonal workspace by assuming that sensing exactly detects when the robot traverses line segments joining vertices of the workspace.

Our notion of a landmark corresponds to a recognizable feature of the workspace that induces a field of influence (the landmark area). If the robot lies in this field, it senses the landmark and uses this information to determine its location. Related notions have been previously introduced in the literature with the same or different names, e.g., landmarks [23], atomic regions [3], signature neighborhoods [26], and perceptual equivalent classes [10, 6]. Over the past decade, there has also been a substantial amount of work at reducing position sensing errors while a robot is moving. For example, for mobile robots, many techniques have been proposed to combine the estimates provided by both dead-reckoning and environmental sensing (e.g., see [1, 7, 22, 33]). These techniques address the problem of tracking a selected motion plan as well as possible, not the problem of generating this plan. The goal of planning in the presence of uncertainty considered in this paper is to make sure that executing the plan will reveal enough information to guarantee reliable execution.

3. PLANNING PROBLEM

In this section we precisely state the class of problems solved by our planning algorithm. We illustrate this statement with a specific example.

3.1. STATEMENT

The robot is a point¹ moving in a plane, the *workspace*, containing stationary forbidden circular regions, the *obstacle disks*. The robot can move in either one of two control modes, the *perfect* and the *imperfect* modes.

The perfect control mode can only be used in some stationary circular areas of the workspace called the *landmark disks*, where the robot also has perfect position sensing. Some of these disks may intersect, creating larger areas, called *landmark areas*, through which the robot can move in the perfect control mode. A motion command in the perfect control mode, called a *P-command*, is described by a sequence of via points such that all the *via points* are in the same landmark area, any two consecutive via points are in the same landmark disk, and any two non-consecutive via points are in different landmark disks. The robot can start executing the command only when it is in the landmark disk containing the first via point. It executes the command by moving through the successive via points and stops when it reaches the last one.

A motion command in the imperfect control mode, called an *I-command*, is described by a pair (d, \mathcal{L}) , where $d \in S^1$ is a direction in the plane, called the *commanded direction of motion*, and \mathcal{L} is a set of landmark disks, called the *termination set* of the command. This command can be executed anywhere in the plane, outside the obstacle disks. The robot then follows a path whose tangent at any point makes an angle with the direction d that is no greater than some prespecified angle $\theta \in (0, \pi/2)$, called the *directional uncertainty*. The robot stops as soon as it enters a landmark disk in \mathcal{L} .

The robot has no sense of time, which means that the modulus of its velocity is irrelevant to the planning problem.

The initial position of the robot is known to be anywhere in a specified *initial region* \mathcal{I} that consists of one or several disks. Each initial-region disk may, or may not be disjoint from the landmark areas. The robot must move into a given *goal region* \mathcal{G}_0 , which is any subset, connected or not, of the workspace whose intersection with the landmark disks is easily computable. The problem is to generate a correct motion plan made up of I- and P-commands to achieve \mathcal{G}_0 from \mathcal{I} . The robot is not allowed to collide with any of the obstacles.

The number of landmark disks is finite and equal to ℓ . The number of obstacle disks is also finite and in $O(\ell)$. The number of initial-region disks is small enough to be considered constant. The goal region is such that its intersection with landmark disks can be computed in $O(\ell)$ time. Hence, ℓ is used to measure the size of the input problem.

The above problem is a simplification of a real mobile-robot navigation problem, but it is not oversimplified and captures most of its fundamental aspects. In Section 8 we will see that the most restricting assumptions can be eliminated or alleviated, so that the methods described in this paper provide a solid foundation for real mobile-robot navigation.

3.2. EXAMPLE

¹Hence, the robot workspace and configuration space coincide.

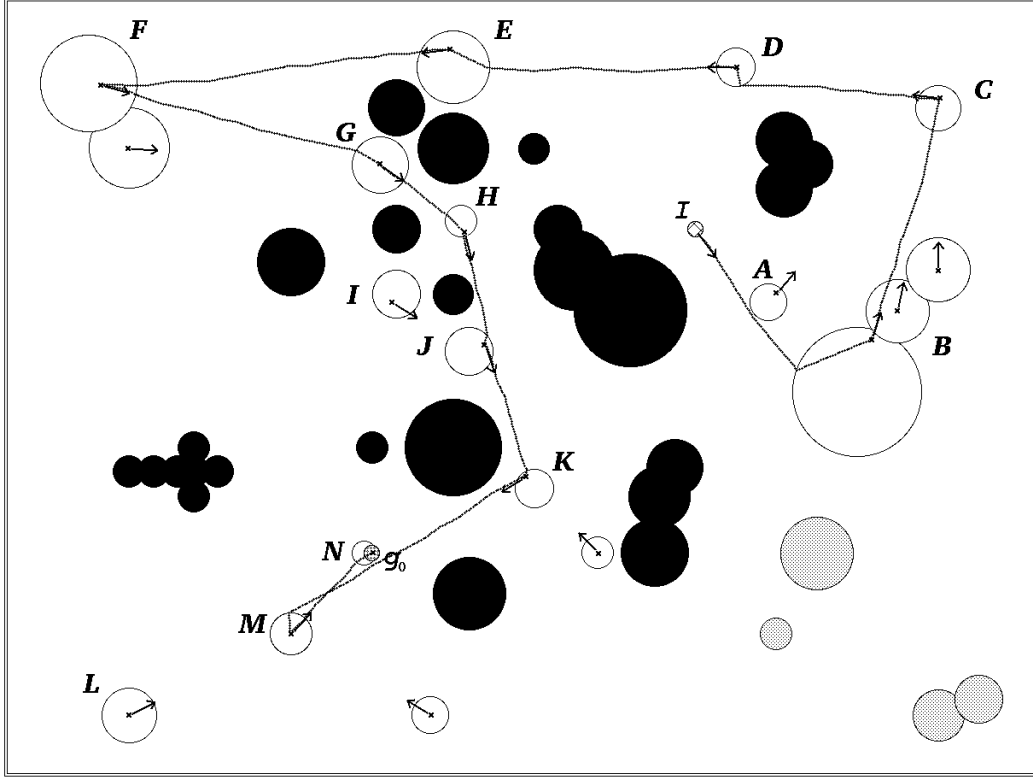


Figure 1: Example of a planning problem

Fig. 1 illustrates the previous description with an example run using the implemented planner. The workspace contains 23 landmark disks (shown white or grey) forming 19 landmark areas, and 25 obstacle disks (shown black). The directional uncertainty θ is set to 0.09 radian. The initial and goal regions are two small disks designated by I and \mathcal{G}_0 , respectively.

The white landmark disks are those with which the planner has associated motion commands. The arrow attached to a white disk is the commanded direction of motion of an I-command planned to attain another set of disks. There is at least one arrow per white landmark area not intersecting the goal.

Plan execution begins with performing the I-command attached to the initial region. When the robot reaches a disk in the termination set of this command, it is guaranteed that a P-command is attached to this disk (hence, it is a white disk in the figure). Executing this P-command allows the robot to attain a point in the current landmark area that is either in the goal (if the goal region intersects this landmark area) or such that an I-command is associated with it (the arrows shown in the figure are drawn from such points). In the first case, plan execution terminates; in the second case, the I-command is executed, and so on.

The figure also shows the path produced by a sample execution of the plan. This path first takes the robot from the initial region to the landmark area designated by B . From there, it successively attains and traverses the landmark areas marked $C, D, E, F, G, H, J, K, M$, and N . The P-command associated with N takes the robot to \mathcal{G}_0 where it stops.

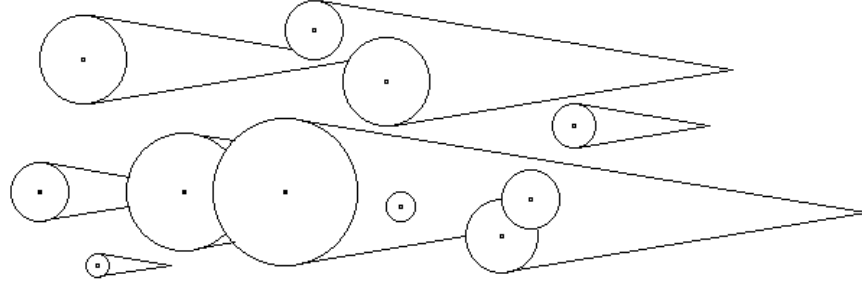


Figure 2: A directional backprojection

The path shown in the figure was produced by the execution of 11 I-commands and 11 P-commands. However, the generated plan could have required up to 12 I-commands. Indeed, the I-command from K is only guaranteed to attain the union of the landmark areas L , M , and N , which form the termination set of the command. Another execution (with different control errors) could have caused the robot to reach L rather than M . The motion command attached to L would then have allowed the robot to reach M .

4. DIRECTIONAL BACKCHAINING

In this section and the next three we assume for simplification that the workspace contains no obstacle disks. Obstacles will be introduced in Section 7.

4.1. DIRECTIONAL BACKPROJECTION OF A GOAL

Consider a goal region \mathcal{G} . We define the *extension* of \mathcal{G} as the largest set of landmark disks such that, if the robot is in any one of them, it can attain the goal by executing a single P-command. Thus, the extension of \mathcal{G} , denoted by $E(\mathcal{G})$, is the set of all the landmark areas having a non-zero intersection with \mathcal{G} . The disks in $E(\mathcal{G})$ are called the *extension disks*. The other landmark disks are called the *intermediate-goal disks*.

The *directional backprojection* of $E(\mathcal{G})$, for any given $d \in S^1$, is the region $B(\mathcal{G}, d)$ defined as the largest subset of the workspace such that, if the robot executes the I-command $(d, E(\mathcal{G}))$ from any position in $B(\mathcal{G}, d)$, then it is guaranteed to reach $E(\mathcal{G})$ and thus to stop in $E(\mathcal{G})$. From the entry point in the extension, the robot can attain \mathcal{G} by executing a P-command. Note that $E(\mathcal{G}) \subset B(\mathcal{G}, d)$. Hence, if the robot is already in $E(\mathcal{G})$ the I-command $(d, E(\mathcal{G}))$ immediately terminates.

There is no larger region than $B(\mathcal{G}, d)$ from where the robot is guaranteed to attain \mathcal{G} recognizably by executing one I-command along d followed by one P-command. Indeed, if the robot executes the I-command $(d, E(\mathcal{G}))$ from any position outside this region, it is not guaranteed to reach $E(\mathcal{G})$. From some positions, it may be guaranteed to reach \mathcal{G} , but since it may not enter any landmark disk intersecting \mathcal{G} , it may not recognize goal achievement and it may thus traverse the goal without stopping.

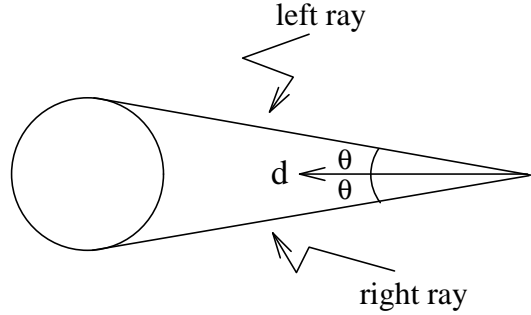


Figure 3: Right and left rays of a landmark disk

4.2. DESCRIPTION OF A DIRECTIONAL BACKPROJECTION

The directional backprojection of a goal extension for any direction $d \in S^1$ consists of one or several connected subsets. Fig. 2 shows a directional backprojection of an 11-disk extension which contains 4 connected subsets.

Each connected subset in $B(\mathcal{G}, d)$ has no hole, even when the union of the extension disks has some. Its boundary consists of circular segments called *arcs* and straight segments called *edges*. Each arc is a subset of the boundary of an extension disk. Let the *right ray* (resp., *left ray*) of an extension disk L be the half-line tangent to L erected from the tangency point in the direction pointed by $\pi + d + \theta$ (resp., $\pi + d - \theta$), with L on its left-hand side (resp., right-hand side), as shown in Fig. 3. Each edge is contained in the right or left ray of some extension disk, and is called a *right* or *left edge*, accordingly. One extremity of the edge, called its *origin*, is the tangency point of the ray. The other extremity, called the edge's *endpoint*, is the first intersection point of the ray with another extension disk or another erected ray. The right (or left) ray of any extension disk thus supports at most one edge of the total backprojection's boundary. If two edges share the same endpoint, this endpoint is called a *spike*. Each connected subset has a single spike.

We assign a distinct integer in $[1, \ell]$ to every landmark disk. Using these numbers we give a distinct *name* to every disk, ray and intersection of two rays.

Except for isolated commanded directions of motion where an edge is tangent to two extension disks or a spike is in contact with an extension disk, every connected subset of a directional backprojection is bounded by a simple curve. We then *label* every edge in the directional backprojection's boundary by the name of the ray supporting it, every arc by the name of the disk it belongs to, and every spike by the name of the corresponding intersection. (Two distinct arcs may receive the same label.) We describe every connected subset of the directional backprojection by the circular list of the labels met along its boundary as it is traced counterclockwisely. The set of all such lists is called the *description* of the directional backprojection. At singular directions, we divide the connected subsets with non-simple boundaries into smaller subsets with simple boundaries that touch each other at isolated points, and we describe each such subset as above.

The extension $E(\mathcal{G})$ contains $O(\ell)$ disks. The size of the boundary of a union of disks is

linear in the number of disks. Hence, the boundary of $E(\mathcal{G})$ contains $O(\ell)$ arcs. Furthermore, the boundary of $B(\mathcal{G}, d)$ contains $O(\ell)$ edges. Indeed, each ray of an extension disk supports at most one edge. So, the size of the description of $B(\mathcal{G}, d)$ is $O(\ell)$. The number of spikes is $O(s)$, where $s \in O(\ell)$ is the number of landmark areas. Thus:

Lemma 1 *The description of a directional backprojection has size $O(\ell)$.*

4.3. COMPUTATION OF A DIRECTIONAL BACKPROJECTION

We assume that the set of all landmark areas has been precomputed. (Computing a landmark area includes identifying its landmark disks, constructing its boundary, and identifying which initial-region disks are fully contained in the area.) The total size of the landmark areas' boundaries is $O(\ell)$. A simple divide-and-conquer does the precomputation in time $O(\ell \log^2 \ell)$ and space $O(\ell)$ [29].

To compute $B(\mathcal{G}, d)$ we erect the $O(\ell)$ rays tangent to the precomputed boundary of $E(\mathcal{G})$ and pointing along the directions $\pi + d \pm \theta$. We construct the boundary of every connected subset of $B(\mathcal{G}, d)$ by sweeping a line perpendicular to d , in the direction of $d + \pi$. Each ray is interrupted where it first intersects an extension disk or another ray. This sweep algorithm requires that $\theta < \pi/2$, in order to guarantee that the robot motion always projects positively on the direction d .

Lemma 2 *The description of a directional backprojection is computed in time $O(\ell \log \ell)$ and space $O(\ell)$.*

4.4. BACKCHAINING

Assume that we select d_0 such that the directional backprojection of the problem's goal \mathcal{G}_0 contains the initial region \mathcal{I} . We then have a motion plan to achieve the goal: From its initial position in \mathcal{I} , the robot can attain the extension $E(\mathcal{G}_0)$ by executing the I-command $(d_0, E(\mathcal{G}_0))$; then, by switching to the perfect control mode, it can reach the goal without leaving $E(\mathcal{G}_0)$.

However, in general, such a “one-step” motion plan does not exist. If $E(\mathcal{G}_0)$ is empty, so is $B(\mathcal{G}_0, d)$ for any $d \in S^1$; in this case, if $\mathcal{I} \not\subseteq \mathcal{G}_0$, the planner can safely return failure. If the extension $E(\mathcal{G}_0)$ is not empty and the backprojection $B(\mathcal{G}_0, d_0)$, for the selected direction d_0 , does not contain \mathcal{I} , we can treat $B(\mathcal{G}_0, d_0)$ as an intermediate goal \mathcal{G}_1 and try to produce a motion plan to achieve it from \mathcal{I} . This means that we compute the extension $E(\mathcal{G}_1)$ and, if it is a proper superset of $E(\mathcal{G}_0)$, the backprojection $B(\mathcal{G}_1, d_1)$ for some direction $d_1 \in S^1$. If we select d_1 such that $B(\mathcal{G}_1, d_1)$ contains \mathcal{I} , we then have a two-step motion plan to achieve \mathcal{G}_0 ; otherwise, we can consider $B(\mathcal{G}_1, d_1)$ as a new intermediate goal \mathcal{G}_2 , and so on. The whole process is called *directional backchaining*.

The backchaining process requires that every newly computed backprojection be checked for containment of the initial region \mathcal{I} . If it does not contain \mathcal{I} , the new backprojection must also be checked for intersection with landmark disks not in the current goal's extension.

These computations can be incorporated in the sweep-line algorithm that constructs the directional backprojection. During the sweep we can remove any intermediate-goal disk from further consideration, as soon as we detect that it is intersected by an edge of the directional backprojection being computed. With this simplification, the time complexity of the sweep-line algorithm remains $O(\ell \log \ell)$.

Let LA be a landmark area in $E(\mathcal{G}_0)$ and G be an arbitrary point selected in $LA \cap \mathcal{G}_0$, called a *goal point*. We construct a tree, called the *P-command tree* of LA , whose nodes are all the disks in LA . The root of the tree is the disk containing G and any two disks related by a link of the tree overlap. (Any tree verifying these properties is adequate.) We select a via point in the intersection of every disk other than the root with its immediate parent in the tree. The P-command tree of LA will be used at execution time to select the P-command to be executed when the robot enters a disk in LA . The P-command will simply be the sequence of via points collected by tracing the path in the tree between the entered disk and the root, with the goal point G added at the end of the sequence. A P-command tree is constructed for every landmark area in $E(\mathcal{G}_0)$.

Consider now the extension $E(\mathcal{G}_i)$ of an intermediate goal \mathcal{G}_i ($i > 0$). In every landmark area $LA \subseteq E(\mathcal{G}_i) \setminus E(\mathcal{G}_{i-1})$, we pick a disk that has a non-zero intersection with \mathcal{G}_i and a point in this intersection. This point is called the *exit point* of LA . In the same way as above, we construct the P-command tree of LA , with the disk containing the exit point as the root. At execution time, if the robot attains this exit point, the generated plan prescribes to immediately switch to executing the I-command $(d_{i-1}, E(\mathcal{G}_{i-1}))$.

A straightforward computation of all the P-command trees takes $O(\ell^2)$ time in total.

5. OMNIDIRECTIONAL BACKCHAINING

In order to transform directional backchaining into an effective planning algorithm, we need a method for choosing a direction of motion at every iteration of the backchaining process. This issue leads to the notion of an omnidirectional backprojection.

5.1. OMNIDIRECTIONAL BACKPROJECTION OF A GOAL

We call the *omnidirectional backprojection* of a goal \mathcal{G} the disjoint union of all directional backprojections over $d \in S^1$, i.e., the three-dimensional set $\bigcup_{d \in S^1} (B(\mathcal{G}, d) \times d) \subset \mathbf{R}^2 \times S^1$. We denote this set by $OB(\mathcal{G})$.

(Remark on terminology: Erdmann [12] defines the *nondirectional backprojection* of a goal as the union of all directional backprojections of this goal over $d \in S^1$. The nondirectional backprojection is thus the two-dimensional set $\bigcup_{d \in S^1} B(\mathcal{G}, d)$. It is the region from where the robot can reach \mathcal{G} by a single move in some direction. Donald [9] employs the same name for the disjoint union of all directional backprojections over d , but the terminology is counter-intuitive. Instead, we use the name “omnidirectional backprojection.”)

At every iteration of the planning process, we wish to compute the omnidirectional backprojection of the current goal in order to answer the following two questions:

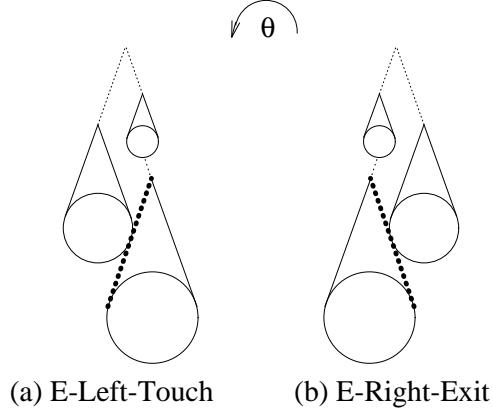


Figure 4: E-events

- Does there exist d such that the initial region \mathcal{I} is contained in the directional backprojection $B(\mathcal{G}, d)$?
- What are all the intermediate-goal disks that are intersected by a directional backprojection in $OB(\mathcal{G})$?

If the answer to the first question is yes, the planning problem is solved. If it is no, the second question tells us which landmark disks, if any, have to be inserted in the new extension for the next backchaining iteration. If there are no such disks, the planner returns failure.

We show below that answering the above questions only requires computing a finite number of directional backprojections in $OB(\mathcal{G})$. Indeed, although there are infinitely many possible values of d , the answers to the above questions change only at a finite number of directions, called *critical directions*.

Let $(d_{c_1}, \dots, d_{c_p})$ be the cyclic list of all critical directions in counterclockwise order and I_1, \dots, I_p be the intervals between them, with $I_i = (d_{c_i}, d_{c_{i+1} \pmod p})$. For any interval I_i , let d_{nc_i} be any direction in I_i . One can answer the above two questions by computing the directional backprojections $B(\mathcal{G}, d)$ for all $d \in \{d_{nc_1}, d_{c_1}, d_{nc_2}, \dots, d_{c_p}\}$. In the following, we will call the set of these backprojections the *discrete omnidirectional backprojection*. We will denote it by $DOB(\mathcal{G})$.

5.2. CRITICAL DIRECTIONS

Assume that d varies over S^1 counterclockwisely. Every critical direction corresponds to an *event* caused by the motion of an edge or a spike of the current directional backprojection relative to the stationary landmark disks or initial-region disks. We assume that all disks are in general position, so that no two events occur simultaneously. Three kinds of events have to be considered:

- E-events, where the directional backprojection changes discontinuously, hence possibly causing the answer to both questions to change. These events involve extension disks only.
- I-events, where the answer to the first question may change. They involve extension and

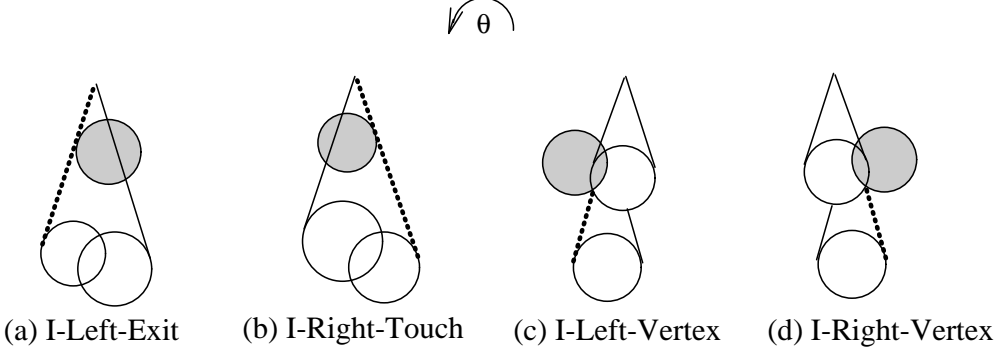


Figure 5: I-events

initial-region disks.

- L-events, where the answer to the second question may change. They involve extension and intermediate-goal landmark disks.

There are two types of E-events (see Fig. 4, where all disks are extension disks):

- An *E-Left-Touch* event occurs when a left edge reaches an extension disk by becoming tangent to it.
- An *E-Right-Exit* event occurs when a right edge leaves the extension disk containing its endpoint by becoming tangent to it.

There are four types of I-events (see Fig. 5, where the grey disk is an initial-region disk):

- An *I-Left-Exit* event occurs when a left edge leaves an initial-region disk by becoming tangent to it.
- An *I-Right-Touch* event occurs when a right edge reaches an initial-region disk by becoming tangent to it.
- An *I-Left-Vertex* event occurs when the endpoint of a left edge coincides with the entry intersection point² of an initial-position disk by an extension disk.
- An *I-Right-Vertex* event occurs when the endpoint of a right edge coincides with the exit intersection point of an initial-position disk by an extension disk.

There are three types of L-events (see Fig. 6, where the dark grey disk is an intermediate-goal disk):

- An *L-Left-Touch* event occurs when a left edge reaches an intermediate-goal disk by becoming tangent to it.
- An *L-Right-Exit* event occurs when a right edge leaves an intermediate-goal disk by becoming tangent to it.
- An *L-Spike-In* event occurs when a spike lies on the boundary of an intermediate-goal disk.

Lemma 3 *There are $O(\ell^2)$ E-Left-Touch and E-Right-Exit events, $O(\ell)$ I-Left-Exit and I-Right-Touch events, $O(\ell^2)$ I-Left-Vertex, I-Right-Vertex, L-Left-Touch, and L-Right-Exit events, and $O(\ell^3)$ L-Spike-In events.*

²When a disk δ_1 intersects another one, δ_2 , we define the *entry intersection point* of δ_2 by δ_1 , as the point where we enter δ_2 when we move counterclockwisely along the boundary of δ_1 . The point where we exit δ_2 is the *exit intersection point*.

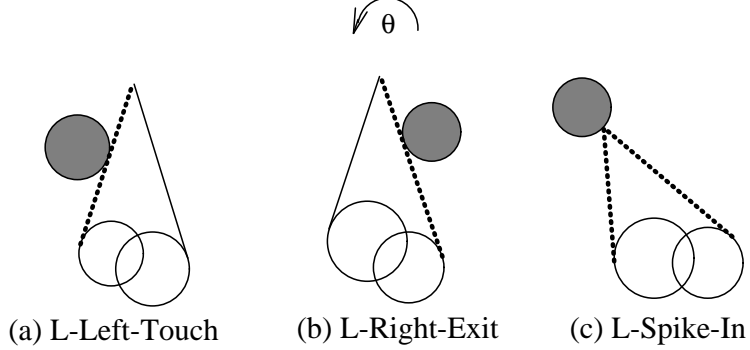


Figure 6: L-events

The curve traced by the intersection of a right and a left ray is a circle if the two rays are tangent to the same disk. Otherwise it is a fourth degree curve. The algebraic expression of the intersection of this curve with a circle is established in [21].

5.3. PLANNING METHOD

If $\mathcal{I} \subset \mathcal{G}_0$, the robot is already in the goal and the planner has nothing to do. In general, however, the planner computes the extension $E(\mathcal{G}_0)$. If this extension is empty, the planner returns failure. Otherwise, it associates a P-command to reach a goal point with every landmark disk in this extension. If $\mathcal{I} \subset E(\mathcal{G}_0)$ the planner returns success.

Let us assume that $\mathcal{I} \not\subset E(\mathcal{G}_0)$. The planner then computes the discrete omnidirectional backprojection $DOB(\mathcal{G}_0)$. If $DOB(\mathcal{G}_0)$ contains a directional backprojection $B(\mathcal{G}_0, d)$ that includes \mathcal{I} , then the planner attaches the I-command $(d, E(\mathcal{G}_0))$ to \mathcal{I} and returns success. Otherwise, for every landmark area $LA \not\subset E(\mathcal{G}_0)$ that has a non-zero intersection with a directional backprojection $B(\mathcal{G}_0, d)$ in $DOB(\mathcal{G}_0)$, an exit point is arbitrarily selected in $LA \cap B(\mathcal{G}_0, d)$ and the I-command $(d, E(\mathcal{G}_0))$ is attached to this point. (If the same area LA intersects several directional backprojections, only one intersection is used to produce the I-command.) The union of the directional backprojections in $OB(\mathcal{G}_0)$ is now considered as an intermediate goal \mathcal{G}_1 .

The extension $E(\mathcal{G}_1)$ is a by-product of the above computation. By construction, $E(\mathcal{G}_1) \supseteq E(\mathcal{G}_0)$. If $E(\mathcal{G}_1) = E(\mathcal{G}_0)$, no directional backprojection of $E(\mathcal{G}_1)$ can possibly intersect a landmark disk that is not already in $E(\mathcal{G}_1)$; hence, the planner terminates with failure. Otherwise, every landmark area in $E(\mathcal{G}_1) \setminus E(\mathcal{G}_0)$ contains one disk L with an exit point and an I-command attached to it. With every other disk in the landmark area, the planner associates a P-command to reach the exit point in L . If $\mathcal{I} \subset E(\mathcal{G}_1)$ the planner returns success, else it computes the discrete omnidirectional backprojection of $E(\mathcal{G}_1)$, and so on.

During this backchaining process, the set of landmark areas in the extensions of the successive goals increases monotonically. At every iteration, either there is a new landmark area in the extension, and the planner proceeds further, or there is no new area, and the planner terminates with failure. The planner terminates with success whenever it has constructed

an extension $E(\mathcal{G}_n)$ containing \mathcal{I} or a discrete omnidirectional backprojection $DOB(\mathcal{G}_n)$ that includes a directional backprojection containing \mathcal{I} . The number of iterations is bounded by the number s of landmark areas. Thus, $n \leq s$. Every iteration of the backchaining process requires computing $O(\ell^3)$ directional backprojections. The computation of a directional backprojection takes time $O(\ell \log \ell)$ (see Subsection 4.3). Hence, the above planning algorithm has time complexity $O(s\ell^4 \log \ell)$.

5.4. PLAN EXECUTION

Assume that the planner returns success after computing an omnidirectional backprojection $OB(\mathcal{G}_n)$ that contains \mathcal{I} . The generated plan can be regarded as a non-ordered collection of *reaction rules* [30]. Each rule is a motion command whose execution is conditional to the entry of the robot into a region of the workspace, either the initial region, or a landmark disk, or an exit point:

- The rule associated with \mathcal{I} is the I-command $(d_n, E(\mathcal{G}_n))$, where d_n is such that $\mathcal{I} \subset B(\mathcal{G}_n, d_n)$.
- The rule associated with a landmark disk is a P-command to attain the exit point or the goal point of the landmark area to which the disk belongs.
- The rule attached to the exit point of each landmark area LA contained in $E(\mathcal{G}_{i+1}) \setminus E(\mathcal{G}_i)$, for any $i \in [0, n - 1]$, is an I-command $(d_i, E(\mathcal{G}_i))$, where d_i is such that $LA \cap B(\mathcal{G}_i, d_i)$ is a non-empty region containing the exit point.

The plan is executed as follows: The robot first executes the I-command associated with the initial region. This command guarantees that the robot will stop in a landmark disk with a P-command attached to it. Then the robot executes this P-command, and attains a goal point or an exit point. If it attains a goal point, the execution of the plan is terminated. If it attains an exit point, the I-command attached to this point is executed. This command leads the robot to a new landmark disk, and so on.

An exit point was selected by the planner in a landmark area when this area intersected a directional backprojection for the first time. Later, the planner never changed the command attached to this point. Therefore, when the robot executes the I-command $(d_i, E(\mathcal{G}_i))$ from the exit point of some landmark area LA , no landmark disk in LA can possibly be in the termination set $E(\mathcal{G}_i)$ of this command. Thus, since $E(\mathcal{G}_0) \subset E(\mathcal{G}_1) \subset \dots \subset E(\mathcal{G}_n)$, the robot cannot terminate its motion in the same landmark area twice by executing the plan. Hence, it is guaranteed to reach \mathcal{G}_0 after executing an alternate sequence of I- and P-commands whose length is smaller than or equal to $2(n + 1)$.

If the planner returns success when $E(\mathcal{G}_n)$ contains \mathcal{I} , the generated plan is essentially the same as above, except that it does not include a rule associated with \mathcal{I} , since the robot will already be in a landmark area having a P-command attached to it.

If the planner returns failure, it still delivers a plan as a set of reaction rules associated with *all* landmark areas from where the goal can be achieved reliably. But the plan is incomplete, since no command is attached to the initial region. The plan can nevertheless be useful. For example, the robot controller may then decide to execute a random motion

until the robot enters a landmark area with a command attached to it (see [21]).

5.5. COMPLETENESS AND OPTIMALITY

By construction, every I-command in a plan is guaranteed to reach a landmark disk in its termination set. Since the robot cannot terminate in the same landmark area twice (see previous subsection), the execution of a plan leads the robot to eventually stop in the goal. Hence, the plans generated by the planner are correct. The planner is sound.

Let us say that a plan has k steps if it contains exactly k I-commands. The extension $E(\mathcal{G}_i)$ of any goal \mathcal{G}_i is the maximal subset of the workspace from which the robot can reliably achieve \mathcal{G}_i in zero steps. The set $\bigcup_{B \in DOB(\mathcal{G}_i)} E(B)$, i.e., the union of the extensions of the directional backprojections in $DOB(\mathcal{G}_i)$, is the maximal subset of landmark disks from which the robot can reliably achieve \mathcal{G}_i in at most one step. Hence, $E(\mathcal{G}_i)$, for any $i \geq 0$, is the maximal set of landmark disks from which the robot can reliably achieve \mathcal{G}_0 in at most i steps. The largest set of landmark disks from where the planner can reliably achieve \mathcal{G}_0 is computed in at most s backchaining iterations. By definition of the I-events, if a directional backprojection of this set contains the initial region, the planner will find one (perhaps before the last iteration). Thus, if \mathcal{G}_0 can reliably be achieved from \mathcal{I} , the planner is guaranteed to terminate with success. If \mathcal{G}_0 cannot reliably be achieved, backchaining terminates with failure after at most s iterations. Thus, the planner is complete.

Let a motion plan be *optimal* if the maximal number of steps required by its execution is minimal over all correct motion plans. The maximal number of steps for a plan produced by our algorithm is equal to the number of backchaining iterations before an extension or a backprojection contains the initial region. By definition of the omnidirectional backprojections, the number of iterations is equal to the minimal number of steps that is required to achieve the goal in the worst case. Hence, our algorithm generates optimal plans. Furthermore, after the execution of any sequence of steps, the subset of the motion plan that may still be used to attain the problem's goal is also optimal.

Theorem 1 *The planning algorithm is complete and generates optimal plans.*

5.6. COMPUTATION IMPROVEMENTS

At every iteration of the backchaining process, the above algorithm identifies critical directions of motion and computes the directional backprojection of the current goal for every such direction. By noticing that the description of a directional backprojection undergoes limited changes between two consecutive directions, we can avoid the full recomputation of each backprojection. To turn this idea into an algorithm, it is necessary to track the variations of the directional backprojection description as the direction d varies along S^1 . It turns out that this description changes only at a finite number of directions caused by the two E-events presented above and other E-events discussed below. At each E-event, except the E-Left-Touch and E-Right-Exit events seen above, the directional backprojection

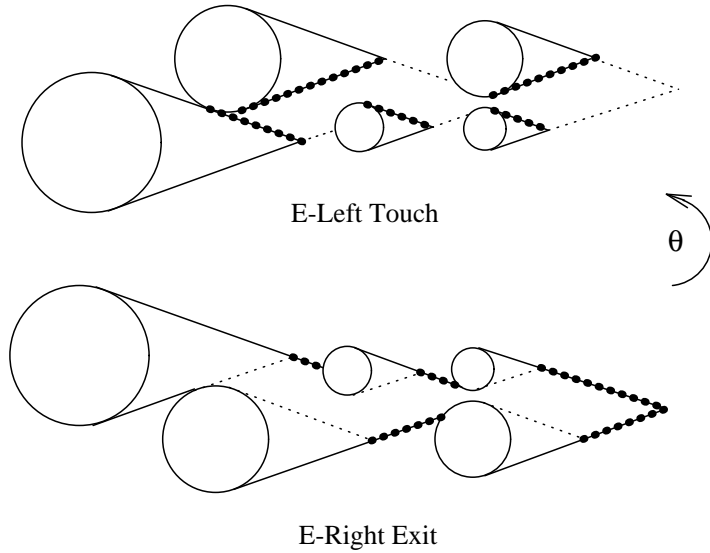


Figure 7: Catastrophic E-Left-Touch and E-Right-Exit events

description undergoes constant change that can be computed in constant or logarithmic time (see below). Meanwhile, E-Left-Touch and E-Right-Exit events, which we call *catastrophic events*, yield $O(\ell)$ changes, as illustrated in Fig. 7.

Hence, the planner can use a sweep algorithm to compute the discrete omnidirectional backprojection. This algorithm scans all potential critical directions in counterclockwise order starting at some non-critical directions where it computes the directional backprojection from scratch. During the sweep, it stops at every critical direction. At non-catastrophic E-events, it simply updates the description of the directional backprojection in constant or logarithmic time. At E-Left-Touch or E-Right-Exit, it recomputes the directional backprojection from scratch. At every I-event, it uses the current backprojection description to determine if the backprojection contains \mathcal{I} . This can be done in a straightforward way in time $O(\ell \log \ell)$. At every L-event, the intersected intermediate-goal disk, if any, is identified in constant time.

The additional E-events where the description of the directional backprojection changes are the following (see Fig. 8):

- An *E-Left-Exit* event occurs when a left edge leaves the extension disk containing its endpoint by becoming tangent to it.
- An *E-Right-Touch* event occurs when a right edge reaches an extension disk by becoming tangent to it.
- An *E-Left-Birth* event occurs when a new left edge emerges at the intersection of two extension disks.
- An *E-Right-Death* event occurs when a right edge disappears at the intersection of two extension disks.
- An *E-Left-Vertex* event occurs when the endpoint of a left edge crosses the intersection between two extension disks.

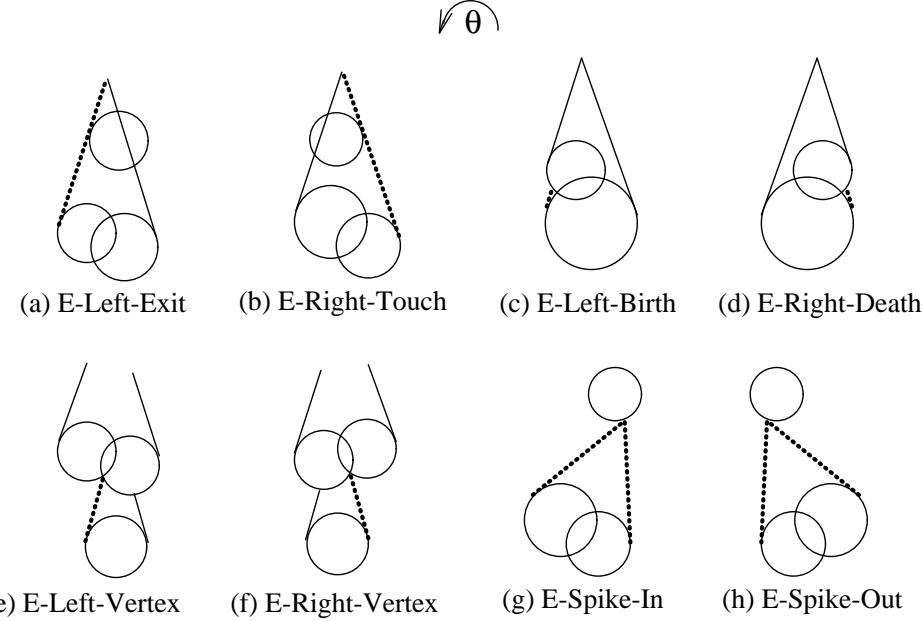


Figure 8: Additional E-events

- An *E-Right-Vertex* event occurs when a right edge crosses the intersection between two extension disks.
- An *E-Spike-In* event occurs when a spike reaches an extension disk.
- An *E-Spike-Out* event occurs when a spike leaves an extension disk.

Lemma 4 *There are $O(\ell)$ E-Left-Birth and E-Right-Death events, $O(\ell^2)$ E-Right-Touch, E-Right-Exit, E-Left-Vertex, E-Right-Vertex events, and $O(\ell^3)$ E-Spike-In and E-Spike-Out events.*

One can easily verify that the directional backprojection undergoes constant change at each of the above E-events. Consider for example an E-Right-Touch event (see Fig. 9). The right ray r of an extension disk is collinear with the right ray r' of another extension disk L' . The description of the directional backprojection is then modified by inserting the names of L' and r' in sequence immediately after the name of r (S^1 is being scanned counterclockwisely). This change takes constant time to compute, as for all non-catastrophic E-events, except E-Spike-In ones. An E-Spike-In event requires the label of the arc touched by the spike to be identified. Its processing takes $O(\log \ell)$ time.

The time complexity of the sweep algorithm is the sum of the time required to schedule the events (i.e., to identify and sort all potential critical directions) and the time to process them. There are $O(\ell^3)$ events in total. Scheduling them takes time $O(\ell^3 \log \ell)$. Processing the $O(\ell^3)$ non-catastrophic E-events takes time $O(\ell^3 \log \ell)$, with the E-Spike-In events dominating this cost. The processing of both the $O(\ell^2)$ catastrophic E-events (these events involve recomputing the directional backprojection description) and the $O(\ell^2)$ I-events also takes

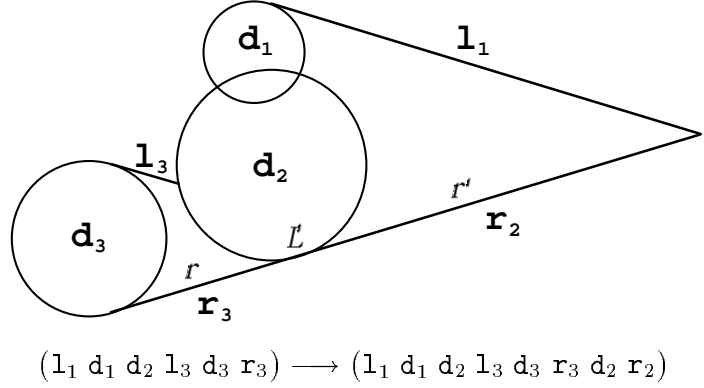


Figure 9: Updating the directional backprojection at an E-Right-Touch event

time $O(\ell^3 \log \ell)$. Processing the $O(\ell^3)$ L-events takes time $O(\ell^3)$. Each iteration of the backchaining process thus takes time $O(\ell^3 \log \ell)$. Hence:

Theorem 2 *The planning algorithm takes time $O(s\ell^3 \log \ell)$ and space $O(\ell^3)$.*

Several simple improvements are possible, which do not change this asymptotic bound. For example, as shown in [21], by considering $O(\ell^2)$ additional I-events, one can process each I-event in constant time, hence reducing the time for processing all I-events to $O(\ell^2)$, instead of $O(\ell^3 \log \ell)$. We also show in [21] that a simple modification of the description of a directional backprojection allows the E-Spike-In and E-Spike-Out events to be eliminated, thus reducing the cost of sorting and processing the non-catastrophic E-events to $O(\ell^2 \log \ell)$. Concerning the L-Spike-In events, we can compute all the $O(\ell^3)$ directions where they may occur in advance, so that we sort them only once and reuse this result at every backchaining iteration. We thus reduce the total time for sorting and processing the L-Spike-In events to $O(s\ell^3)$. The $O(s\ell^3 \log \ell)$ time complexity of the planner is then only dominated by the processing of the $O(\ell^2)$ catastrophic E-events.

6. EXPERIMENTAL RESULTS

We have implemented the above planning algorithm, along with navigation techniques and a robot simulator, in C on a DECstation 5000. The implemented planner incorporates two significant improvements:

(1) During the computation of an omnidirectional backprojection, it does not discard an intermediate-goal disk L as soon as this disk intersects a directional backprojection. Instead, it determines the intervals of all directions at which the directional backprojection intersects L , computes the intersection of L with the directional backprojection at the midpoint of each such interval, and keeps the intersection having the biggest area. This intersection is called the *exit region* of L .

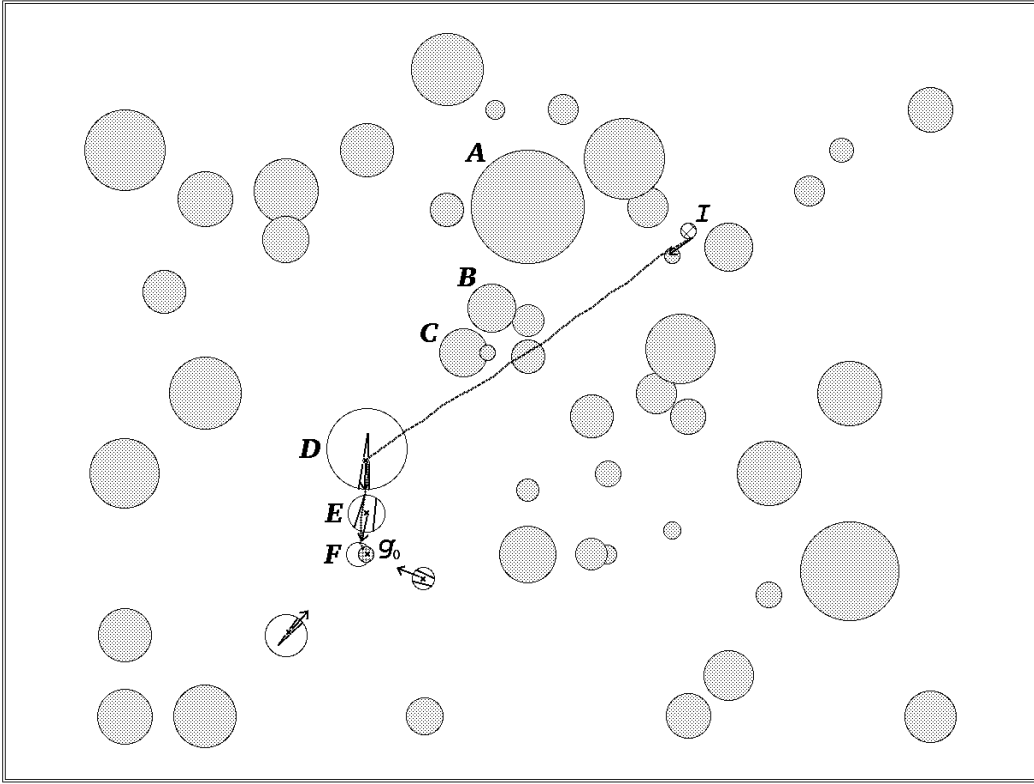


Figure 10: Example with $\theta = 0.1$ radian

(2) Several exit regions, each in a unique disk, may be generated in the same landmark area. With each disk in such a landmark area, the planner associates a P-command leading to one exit region constructed in the area. When several exit regions are available, it selects the region that allows the generation of the P-command containing the smallest number of via points.

The purpose of the first modification is to allow some errors in control and sensing in the landmark areas (see Subsection 8.2). The second modification avoids planning P-commands through long sequences of disks in a landmark area when this is not necessary. (However, it is only a heuristic, since it does not take the radii of the landmark disks into account.)

Below we present examples of plans generated by the implemented planner, along with their simulated execution. In all the figures (for instance, see Fig. 11) white disks are landmark disks that intersect the omnidirectional backprojections computed by the planner, except the last one, i.e., the one that includes the initial region (if such a backprojection exists). Grey disks are the other landmark disks and no command is attached to them. In all examples, there is a single initial-region disk designated by \mathcal{I} , and a single goal-region disk designated by \mathcal{G}_0 .

Whenever the robot enters a new landmark area L that is part of the termination set of the I-command currently being executed (then the disks in L are necessarily white), it shifts to executing a P-command leading to a point (the exit point) selected in an exit region in L ;

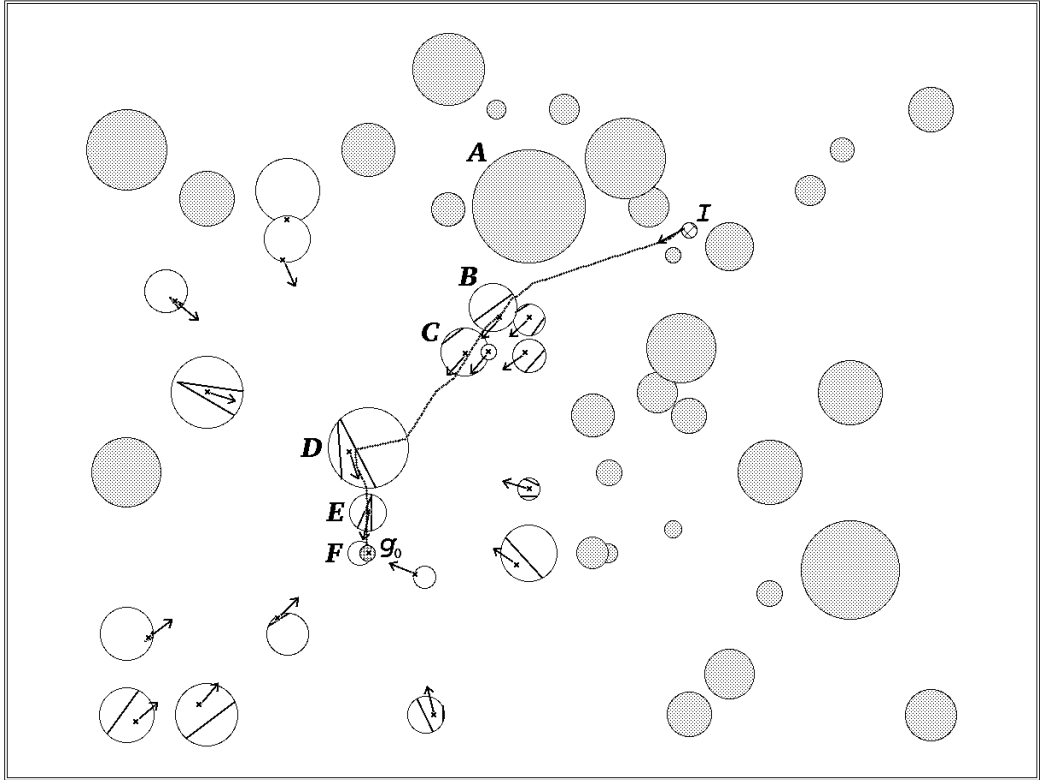


Figure 11: Example with $\theta = 0.2$ radian

as soon as it enters the exit region containing the exit point, it abandons the P-command and shifts to executing the corresponding I-command attached to the exit point. The exit region constructed in every white disk, if there is one such region, is shown in the figures (except when it covers the whole disk), together with the direction of the I-command attached to the selected exit point. The termination sets of the I-commands are not shown in the figure, but can be inferred from the drawings.

Fig. 10, 11, and 12 display three examples with the same workspace containing 51 landmark disks of various size and the same initial and goal regions, but with increasing directional uncertainty θ . These examples show that, when uncertainty grows, the planner returns more and more sophisticated plans, as it attempts to reduce uncertainty by leading the robot through additional landmark disks.

In Fig. 10 we set θ to 0.1 radian. The planner returned success after 2 iterations and less than 3 seconds of computation time. Because the directional uncertainty is small, the plan is almost directly aimed toward the goal. The simulated execution produces a path traversing a single landmark disk designated by D before entering the goal extension. Although the disk marked E is along the path between D and F , it is not in the termination set of the I-command executed from the exit point of D . The robot traverses E without shifting to another motion command.

In Fig. 11 we set θ to 0.2 radian. It took 4 iterations of the planner, and 19 seconds of

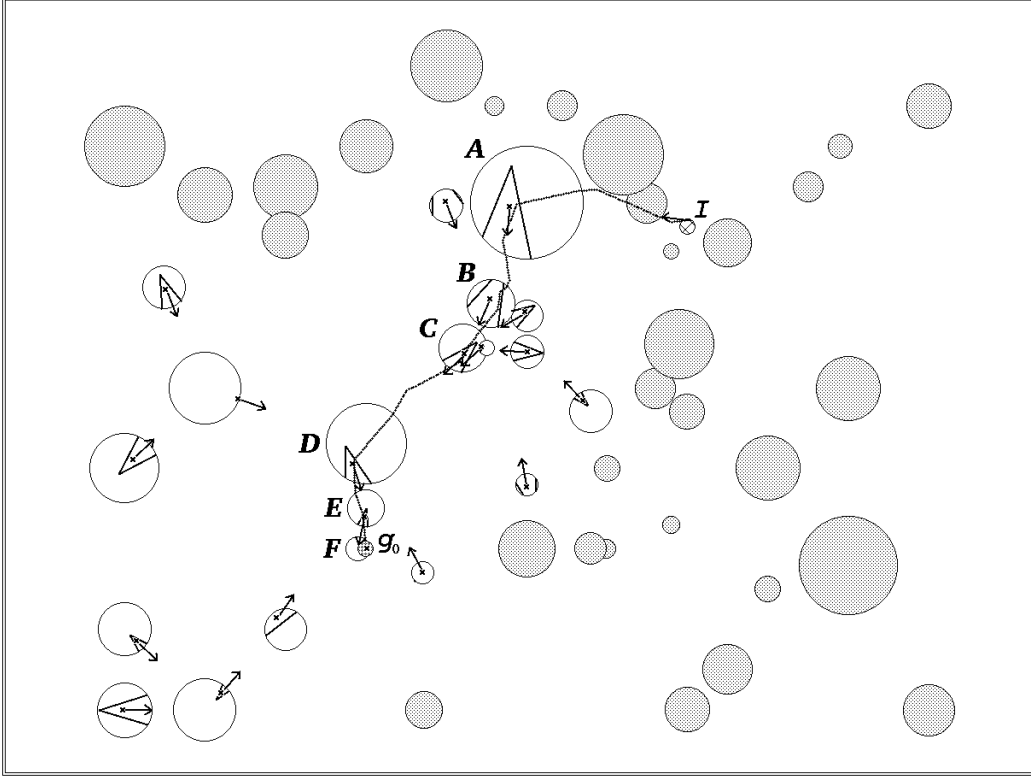


Figure 12: Example with $\theta = 0.3$ radian

computation, before the initial region was included in a backprojection. In the process, the planner attached motion commands to many landmark disks. The simulated execution of the plan produced a path that uses three successive landmark areas designated by B , D , and E , before entering the goal's extension (F). The area C is also traversed by the path, but it is not part of the termination set of the I-command executed from B .

In Fig. 12 we set θ to 0.3 radian. A plan was generated after 6 iterations, and 52 seconds of computation. A quick comparison of the commanded directions of motion attached to the white landmark disks shows that this plan is quite different from the plan of Fig. 11. The executed path traverses 5 landmark areas designated by A , B , C , D , and E . Notice that both B and C are now used by the navigation system, because it is no longer reliable to directly achieve D from B ; C has to be used along the way to reduce uncertainty.

7. DEALING WITH OBSTACLES

Let us now introduce $O(\ell)$ forbidden circular regions, the obstacle disks, in the workspace. We assume for simplicity that these disks have null intersection with the landmark and initial-region disks, and do not even touch them. (Retracting this assumption presents no particular difficulty, but increases the number of event types to be considered.)

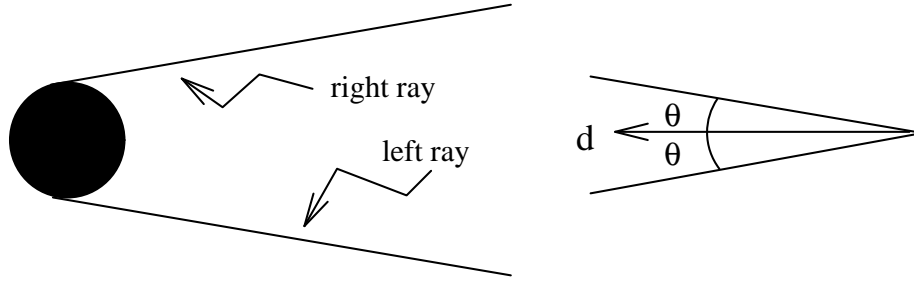


Figure 13: Right and left rays of an obstacle disk

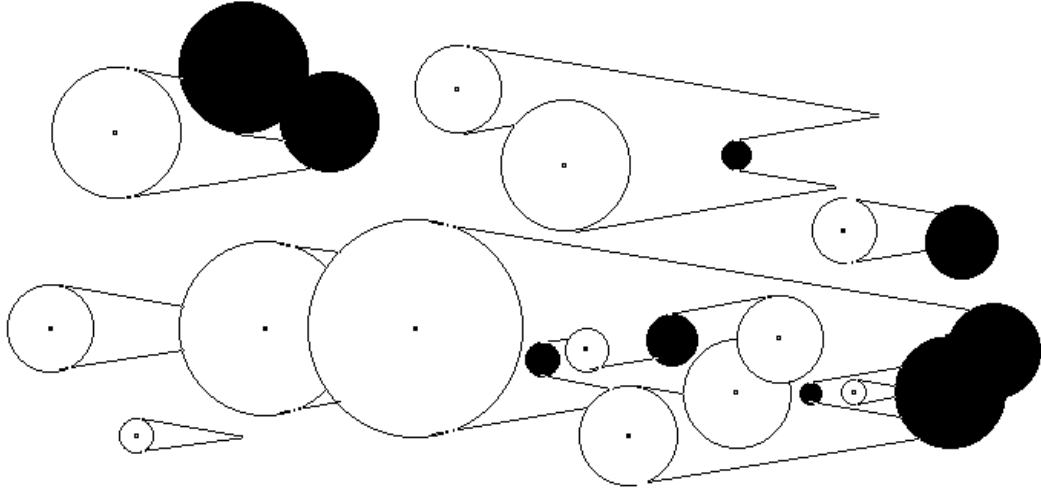


Figure 14: Directional backprojection in the presence of obstacle disks

7.1. DIRECTIONAL BACKPROJECTION DESCRIPTION

Let us consider an obstacle disk B and a commanded direction of motion d . We define the *right ray* (resp., *left ray*) of B as the half-line tangent to B drawn from the tangency point in the direction $\pi + d + \theta$ (resp., $\pi + d - \theta$), with the obstacle on its right-hand side (resp., left-hand side), as shown in Fig. 13.

The directional backprojection of a goal in the presence of obstacle disks is a region bounded by arcs and edges. Each arc is a subset of the boundary of an extension or obstacle disk. Each edge is a line segment supported by the right or left ray of an extension or obstacle disk. When an edge intersects an extension disk L , the edge is terminated and L is included in the backprojection. When an edge intersects an obstacle disk B , the ray is also interrupted, but B is excluded from the backprojection. Fig. 14 shows an example of such a directional backprojection. Extension disks are shown white, while obstacle disks are shown black. Notice that the backprojection may now contain holes, which themselves may contain components of the backprojection. Moreover, its connected subsets may have zero, one, or several spikes. The total number of edges and arcs in the backprojection's boundary is still in $O(\ell)$.

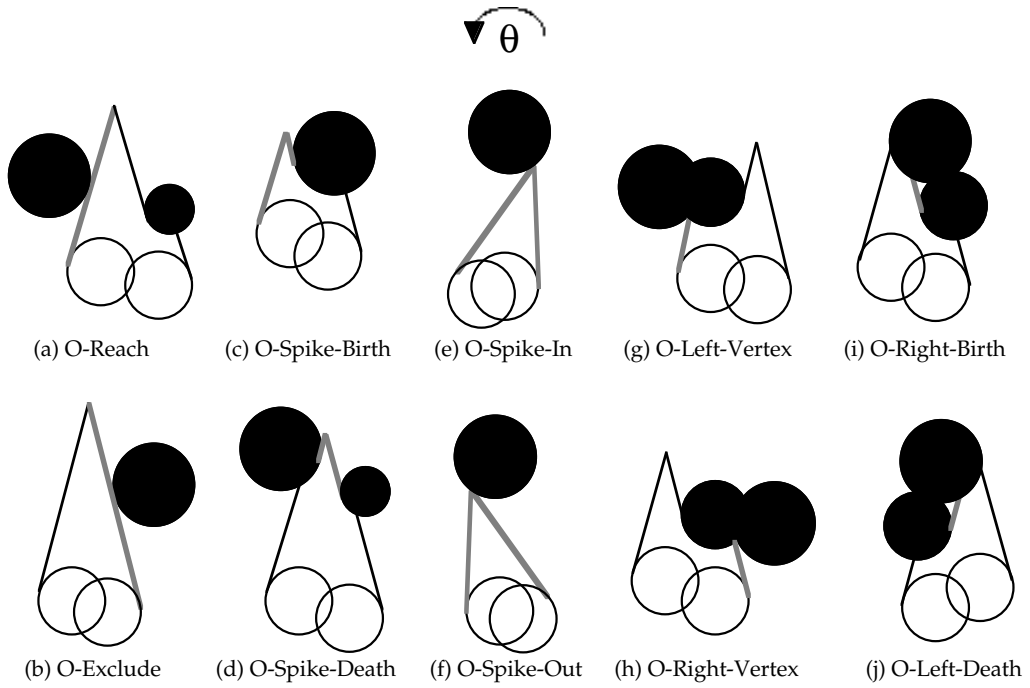


Figure 15: Events caused by obstacle disks

We construct the description of a directional backprojection very much in the same way as when there are no obstacles. We simply give a name to every obstacle disk so that we can label the various edges and arcs of the backprojection’s boundary that arise from the presence of the obstacles. Although there are more types of labels to handle, the computation of this description still takes time $O(\ell \log \ell)$.

Lemma 5 *The description of a directional backprojection in the presence of $O(\ell)$ obstacles is computed in time $O(\ell \log \ell)$ and space $O(\ell)$.*

7.2. CRITICAL DIRECTIONS DUE TO OBSTACLES

When the commanded direction of motion varies counterclockwisely over S^1 , the obstacle disks cause the description of the directional backprojection of a set of landmark disks to change at critical directions corresponding to the following events (see Fig. 15, where extension disks are shown white and obstacle disks are shown black):

- An *O-Left-Touch* event occurs when a left edge reaches an obstacle disk by becoming tangent to it.
- An *O-Right-Exit* event occurs when a right edge leaves an obstacle disk by becoming tangent to it.
- An *O-Spike-Birth* event occurs when a spike emerges as a left edge terminating on an

obstacle disk reaches the point where a right edge arises from this disk.

- An *O-Spike-Death* event occurs when a spike vanishes as its left edge, pushed by its right edge, shortens to zero length against an obstacle disk.
- An *O-Spike-In* event occurs when a spike enters an obstacle disk.
- An *O-Spike-Out* event occurs when a spike exits an obstacle disk.
- An *O-Left-Vertex* event occurs when the endpoint of a left edge reaches the intersection of two obstacle disks.
- An *O-Right-Vertex* event occurs when the endpoint of a right edge reaches the intersection of two obstacle disks.
- An *O-Right-Birth* event occurs when a right edge emerges at the intersection of two obstacle disks.
- An *O-Left-Death* event occurs when a left edge disappears at the intersection of two obstacle disks.

Lemma 6 *There are $O(\ell)$ events of types *O-Right-Birth* and *O-Left-Death*, $O(\ell^2)$ events of types *O-Left-Touch*, *O-Right-Touch*, *O-Spike-Birth*, *O-Spike-Death*, *O-Right-Vertex*, *O-Left-Vertex*, and $O(\ell^3)$ events of types *O-Spike-In* and *O-Spike-Out*.*

7.3. COMPUTATION

The directional backprojection undergoes a small change at each of the above events. This change is computed in constant time for all events. Therefore, the discrete omnidirectional backprojection in the presence of obstacle disks still requires $O(\ell^3 \log \ell)$ to compute, and the time complexity of the planning algorithm remains $O(s\ell^3 \log \ell)$. The space complexity also remains $O(\ell^3)$. Hence:

Theorem 3 *The planning algorithm in the presence of $O(\ell)$ obstacle disks takes time $O(s\ell^3 \log \ell)$ and space $O(\ell^3)$.*

7.4. EXPERIMENTAL RESULTS

Fig. 1 displays both an example of a plan generated by the planner and a sample run of this plan. Obstacle disks are black. Landmark disks are white or grey depending on whether a reaction rule has been attached to them, or not. The initial region is the disk \mathcal{I} . The goal region is the disk \mathcal{G}_0 . In this example, θ was set to 0.09 radian. The generation of the plan took 12 iterations of the planner, and about 3.5 minutes of computation.

Fig. 16 shows another example with the same landmark and obstacle disks (except for 3 obstacles disks that have been removed) and θ set to 0.1 radian. This example was solved after 6 iterations (the displayed path has only 5 steps) requiring 40 seconds of computation.

Fig. 17 shows a third example with a different workspace containing 34 landmark disks forming 28 landmark areas, and 37 obstacle disks. It was solved in 7 iterations (the displayed path also has 7 steps) and less than 6 minutes of computation.

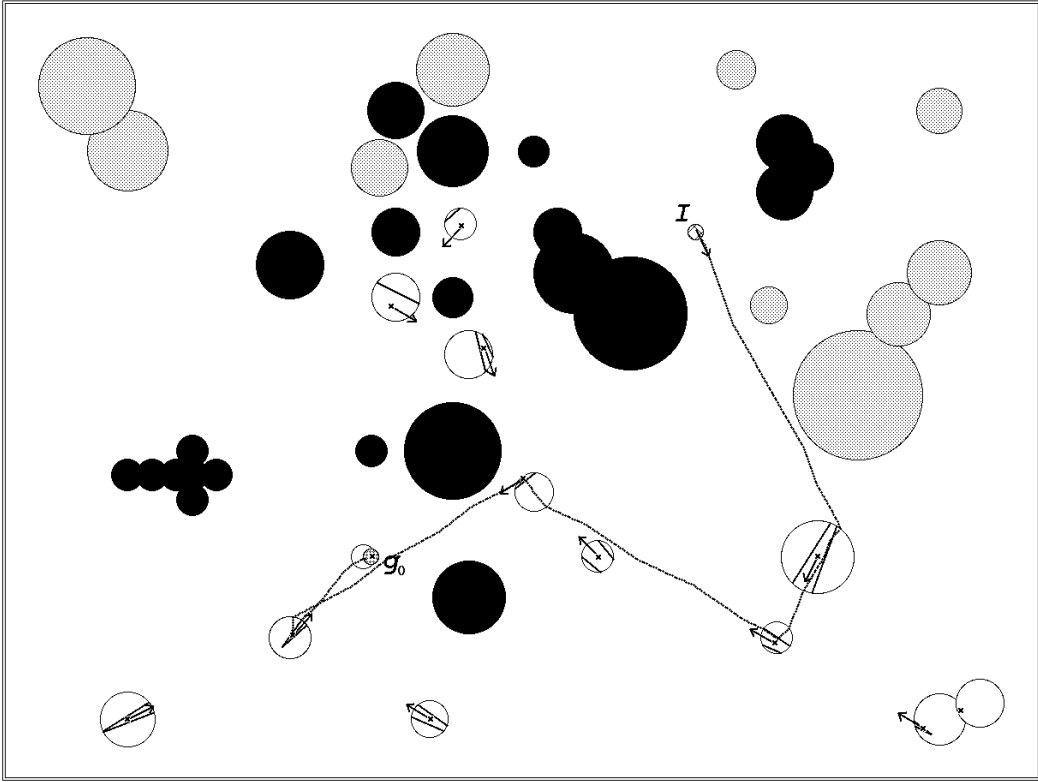


Figure 16: Example with obstacles ($\theta = 0.1$ radian)

8. DISCUSSION AND EXTENSIONS

In this section we discuss non-implemented extensions of the planner.

8.1. LANDMARK AND OBSTACLE GEOMETRY

In the algorithm described above, the landmark and obstacle areas are unions of circular disks. We initially chose to model the fields of influence of the landmarks by disks because we had in mind some sorts of beacons (e.g., radio or infra-red beacons) to guide the robot. For uniformity, we made the same choice for the obstacles. However, most natural landmarks do not entail circular fields of influence. We can approximate any landmark or obstacle area by a collection of overlapping disks, but the number of these disks grows quickly with the precision of the approximation, yielding longer computation.

Our algorithm can be easily adapted to deal with landmark and obstacle areas described as generalized polygonal regions bounded by straight and circular edges. In this extension, for any commanded direction of motion, we can still define the right and left rays of a landmark or an obstacle area. If the area is not convex, it may have several right and/or left rays. While the origin of the right or left ray of a circular contour varies continuously as the commanded direction of motion rotates, the origin of the right or left ray of a polygonal contour remains

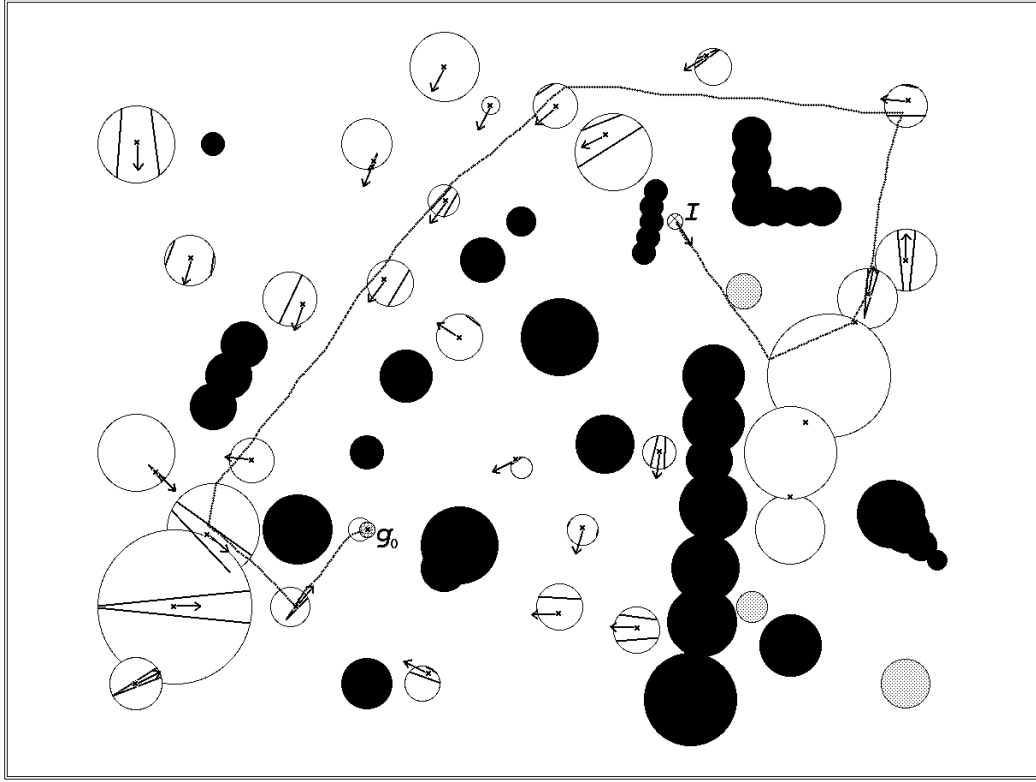


Figure 17: Another example with obstacles ($\theta = 0.1$ radian)

anchored at a fixed vertex, except at critical directions where it jumps from one vertex of the contour to another. These directions (which are parallel to the straight edges of the generalized polygonal contours of the landmark and obstacle areas) are additional critical directions to be treated by the planner. Also, if an extension landmark area and an obstacle area touch each other, we may have to erect a ray whose origin is an intersection point of the two contours. The origin of such a ray remains stationary for a subrange of orientations d . The curves traced by the spikes are not more complicated than in the pure circular case and their degrees remain no greater than 4.

Although several small adaptations have to be carefully made, our planning method thus extends to the case where landmark and obstacle areas are bounded by straight edges and circular arcs and may touch each other. If the workspace contains s landmark areas bounded by $O(\ell)$ edges and arcs and the obstacle areas are bounded by $O(\ell)$ edges and arcs, the time complexity of the planner remains $O(s\ell^3 \log \ell)$.

Representing landmark and obstacle areas as generalized polygons is a very realistic model for most applications. In particular, if the robot is an omnidirectional circular robot moving among polygonal obstacles, shrinking the robot to its centerpoint and growing the obstacles isotropically by the robot's radius yields such generalized polygonal regions.

In a similar way, the algorithm can be extended to allow compliant motions on obstacle

edges. Additional critical directions must be considered by the planner, but complexity bounds remain unchanged. Allowing compliance significantly enlarges the set of problems that admit correct plans.

8.2. UNCERTAINTY IN LANDMARK AREAS

Perhaps the less realistic assumption in the problem definition of Section 3 is that control and position sensing are perfect in landmark areas, while sensing is null outside any such area. Below, we first argue that this assumption is reasonable. We then show that it can be relaxed to some extent.

A typical mobile robot uses two techniques to continuously estimate its position, dead-reckoning and environmental sensing. Environmental sensing provides pertinent information only when some characteristic features of the workspace (“landmarks”) are visible by the sensors. Then the robot knows its position with a good accuracy. When no or few features are visible, the robot relies on dead-reckoning, which yields cumulative errors that we model by the directional uncertainty. Our assumption that sensing outside landmark areas is null is perhaps conservative, but it does not prevent the robot’s navigation system from using all available sensing information at execution time to better determine the robot’s current position. In the worst case, this may lead the planner to return failure, while reliable paths exist in practice.

On the contrary, the assumption that control is perfect in the landmark areas is anti-conservative; but if we choose safe features to create landmark disks, it is a reasonable one. To some extent, most workspaces can be engineered to include such features. Landmark areas with sharp boundaries can be obtained by introducing artificial landmarks and/or thresholding an estimate of the sensing uncertainty. For example, the notion of a “sensory uncertainty field” (SUF) is introduced in [31]. At every possible point q in the configuration space, the SUF estimates the range of possible errors in the sensed configuration that the navigation system would compute by matching the sensory data against a prior model of the workspace, if the robot was at q . The SUF is computed at planning time from a model of the robot’s sensing system.

More interestingly, however, one can notice that perfect control and sensing in landmark areas are not strictly needed. Indeed, once the robot enters a landmark area it is sufficient that it reaches an exit region of non-zero measure prior to executing the next I-command. (If the landmark area intersects the goal, the “exit region” is the intersection with the goal.) For example, the maximal sensing error allowed in a landmark area could be half the radius of the largest disk fully contained in an exit region. Thus, although the planner assumed perfect sensing in landmark areas, we can now create these areas by engineering the workspace in such a way that the sensors just provide the information that is needed by the plan (see [13] for a similar idea). However, maximal errors in landmark areas seem to depend on the plan itself, so that they can only be computed once a plan has been generated assuming no such errors.

8.3. OTHER TYPES OF LANDMARKS

One can define other, perhaps more realistic types of landmarks, which only require simple adaptations of our planning algorithm.

An example of another type of landmark area is a region L containing a subregion C , such that if the robot ever enters L , it knows that it is in L and it can reliably navigate into C ; when it enters C , it recognizes the achievement of C . This definition does not require perfect control in L , nor perfect position sensing. For example, consider a wall w and the corner it makes with another wall. The wall w induces an area L , such that if the robot is in L , its proximity sensor can sense the wall (we assume that w cannot be confused with another object). If the robot moves along w , parallel to it (e.g., using proximity sensing), toward the corner, it will eventually reach a small region C from where it can sense the corner.

A landmark area (L, C) as above can be treated by our algorithm as follows: In order for a directional backprojection to “intersect” this landmark area, it has to fully contain C (yielding events similar to the I-events used for containment of the initial region). When this is the case the whole region L can be inserted in the goal extension used at the next backchaining iteration.

A particular case of the above landmark is when $C = L$. For example, a characteristic feature defines an area L from where it can be sensed. If the feature is not sufficient to allow the robot to determine its location or navigate into a subregion of L , we can simply set $C = L$. Then the only information used by the planner is: if the robot ever enters L , it will know it.

9. CONCLUSION

This paper described a complete polynomial planning algorithm for mobile-robot navigation in the presence of uncertainty. The algorithm addresses a class of problems where landmarks create regions in the configuration space where both control and position sensing are perfect. Outside these regions sensing is null; control, which relies on dead-reckoning, is imperfect, but directional errors are bounded. Although this class of problems is a simplification of real mobile-robot planning problems, by no means it is oversimplified.

A computer program embedding the planning algorithm was implemented, along with navigation techniques and a robot simulator. This program was run with many different examples, some of which were presented in this paper. The planner is reasonably fast. In its present form, it assumes that all landmark and obstacle areas are described as unions of disks. However, extending the planner to accept a more general geometry (generalized polygonal areas) is rather straightforward. Other interesting extensions (uncertainty in landmark areas, new types of landmark areas) are possible. The relative time efficiency of the planner suggests that our complexity bounds are not tight.

So far, most algorithms to plan motion strategies under uncertainty were either exponential in the size of the input problem, unsound, and/or incomplete. Such algorithms may

be interesting from a theoretical point of view, but their computational complexity or lack of reliability prevent them from being applied to real-world problems. Our work shows that it is possible to identify a restricted, but still realistic, subclass of planning problems that can be solved in polynomial time. This subclass is obtained through assumptions whose satisfaction may require prior engineering of the robot and/or its workspace. In our case, this implies the creation of adequate landmarks, either by taking advantage of the natural features of the workspace, or introducing artificial beacons, or using specific sensors. We call this type of simplification *engineering for planning tractability*.

Engineering the robot and the workspace has its own cost and we would like to minimize it. Therefore, future research should aim at finding more general classes of problems than the one solved by the current planner, but requiring less engineering and still solvable in polynomial time. It should also investigate the following “inverse” problem: Given our planning method and the description of a family of tasks (e.g., the set of all possible initial and goal regions), how to minimally engineer the workspace? For instance: What is the minimal number of landmarks that we should place in the workspace and where should we place them, so that every possible problem admits a correct plan?

References

- [1] Ayache, N., *Artificial Vision for Mobile Robots: Stereo Vision and Multisensory Perception*, The MIT Press, Cambridge, MA, 1991.
- [2] Briggs, A.J., “An efficient Algorithm for One-Step Planar Compliant Motion Planning with Uncertainty,” *Proc. of the 5th Annual ACM Symp. on Computational Geometry*, Saarbruchen, Germany, 1989, pp. 187-196.
- [3] Buckley, S.J., *Planning and Teaching Compliant Motion Strategies*, Ph.D. Dissertation, Department of Electrical Engineering and Computer Science, MIT, Cambridge, MA, 1986.
- [4] Canny, J.F. and Reif, J., “New Lower Bound Techniques for Robot Motion Planning Problems,” *27th IEEE Symposium on Foundations of Computer Science*, Los Angeles, CA, 1987, pp. 49-60.
- [5] Canny, J.F., “On Computability of Fine Motion Plans,” *Proc. of the IEEE Int. Conf. on Robotics and Automation*, Scottsdale, AZ, 1989, pp. 177-182.
- [6] Christiansen, A., Mason, M. and Mitchell, T.M., “Learning Reliable Manipulation Strategies without Initial Physical Models,” *Proc. of the IEEE Int. Conf. on Robotics and Automation*, Cincinnati, OH, 1990, pp. 1224-1230.
- [7] Crowley, J.L., “World Modeling and Position Estimation for a Mobile Robot Using Ultrasonic Ranging,” *Proc. of the IEEE Int. Conf. on Robotics and Automation*, Scottsdale, AZ, 1989, pp. 674-680.
- [8] Donald, B.R., “A Geometric Approach to Error Detection and Recovery for Robot Motion Planning with Uncertainty,” *Artificial Intelligence J.*, 37(1-3), 1988, pp. 223-271.

- [9] Donald, B.R., "The Complexity of Planar Compliant Motion Planning Under Uncertainty," *Algorithmica*, 5, 1990, pp. 353-382.
- [10] Donald, B.R. and Jennings, J., "Sensor Interpretation and Task-Directed Planning Using Perceptual Equivalence Classes," *Proc. of the IEEE Int. Conf. on Robotics and Automation*, Sacramento, CA, 1991, pp. 190-197.
- [11] Dufay, B. and Latombe, J.C., "An Approach to Automatic Robot Programming Based on Inductive Learning," *Int. J. of Robotics Research*, 3(4), 1984, pp. 3-20.
- [12] Erdmann, M., **On Motion Planning with Uncertainty**, Tech. Rep. 810, AI Lab., MIT, Cambridge, MA, 1984.
- [13] Erdmann, M., **Towards Task-Level Planning: Action-Based Sensor Design**, Tech. Rep. CMU-CS-92-116, Dept. of Computer Science, Carnegie Mellon Univ., Pittsburgh, PA, February 1992.
- [14] Fox, A. and Hutchinson, S., **Exploiting Visual Constraints in the Synthesis of Uncertainty-Tolerant Motion Plans**, Tech. Rep. UIUC-BI-AI-RCV-92-05, The University of Illinois at Urbana-Champaign, October 1992.
- [15] Friedman, J., **Computational Aspects of Compliant Motion Planning**, Ph.D. Dissertation, Tech. Rep. No. STAN-CS-91-1368, Dept. of Computer Science, Stanford University, Stanford, CA, 1991.
- [16] Gottschlich, S.N. and Kak, A.C., "Dealing with Uncertainty in CAD-Based Assembly Motion Planning," *Proc. of the 9th Nat. Conf. on Artificial Intelligence*, Anaheim, CA, July 1991, pp. 646-652.
- [17] Hutchinson, S., "Exploiting Visual Constraints in Robot Motion Planning," *Proc. of the IEEE Int. Conf. of Robotics and Automation*, Sacramento, CA, 1991, pp. 1722-1727.
- [18] Latombe, J.C., **Robot Motion Planning**, Kluwer Academic Publishers, Boston, MA, 1991.
- [19] Latombe, J.C., Lazanas, A., and Shekhar, S., "Robot Motion Planning with Uncertainty in Control and Sensing," *Artificial Intelligence J.*, 52(1), 1991, pp. 1-47.
- [20] Laugier, C. and Théveneau, P., Planning Sensor-Based Motions for Part-Mating Using Geometric Reasoning Techniques, *Proc. of European Conf. on Artificial Intelligence*, Brighton, UK, 1986.
- [21] Lazanas, A., and Latombe, J.C., **Landmark-Based Robot Navigation**, Tech. Rep. STAN-CS-92-1428, Dept. of Computer Science, Stanford, CA, 1992.
- [22] Leonard, J.J. and Durrant-Whyte, H.F., "Mobile Robot Localization by Tracking Geometric Beacons," *IEEE Tr. on Robotics and Automation*, 7(3), 1991, pp. 376-382.
- [23] Levitt, T.S., Lawton, D.T., Chelberg, D.M. and Nelson, P.C., "Qualitative Navigation," *Image Understanding Workshop*, Los Angeles, CA, 1987, pp. 447-465.
- [24] Lozano-Pérez, T., **The Design of a Mechanical Assembly System**, Tech. Rep. AI-TR 397, Artificial Intelligence Laboratory, MIT, 1976.
- [25] Lozano-Pérez, T., Mason, M.T. and Taylor, R.H., "Automatic Synthesis of Fine-Motion Strategies for Robots," *Int. J. of Robotics Research*, 3(1), 1984, pp. 3-24.

- [26] Mahadevan, S. and Connell, J., **Automatic Programming of Behavior-based Robots using Reinforcement Learning**, Research Rep., IBM T.J. Watson Research Center, Yorktown Heights, NY, 1990.
- [27] Mason, M.T., “Automatic Planning of Fine Motions: Correctness and Completeness,” *Proc. of the IEEE Int. Conf. on Robotics and Automation*, Atlanta, GA, 1984, pp. 492-503.
- [28] Natarajan, B.K., “The Complexity of Fine Motion Planning,” *Int. J. of Robotics Research*, 7(2), 1988, pp. 36-42.
- [29] Preparata, F.P. and Shamos, M.I., **Computational Geometry: An Introduction**, Springer Verlag, New York, 1985.
- [30] Schoppers, M.J., **Representation and Automatic Synthesis of Reaction Plans**, Ph.D. Dissertation, Dept. of Computer Science, University of Illinois at Urbana-Champaign, Urbana, IL, 1989.
- [31] Takeda, H. and Latombe, J.C., “Sensory Uncertainty Field for Mobile Robot Navigation,” *Proc. of the IEEE Int. Conf. on Robotics and Automation*, Nice, France, 1992, pp. 2465-2472.
- [32] Taylor, R.H., **Synthesis of Manipulator Control Programs from Task-Level Specifications**, Ph.D. Dissertation, Department of Computer Science, Stanford University, 1976.
- [33] Zhang, Z. and Faugeras, O., “A 3D World Model Builder with a Mobile Robot,” *The Int. J. of Robotics Research*, 11(4), 1992, pp. 269-285.